Sustainable Synthesis of Multifunctional Zinc Ferrite Nanoparticles Using Date Seed Extract for Antibacterial and Antioxidant Applications

Duaa J. Kadhim and Mahdi A. Mohammed
Department of Physics, College of Science, Wasit University, 52001 Al-Kut, Iraq
std2024204.duaarajaa@uowasit.edu.iq

Keywords: Green Synthesis, $ZnFe_2O_4$ Nanoparticles, Date Seeds, Antibacterial Activity, Antioxidant Activity.

Abstract: This research presents the synthesis of zinc ferrite ($ZnFe_2O_4$) nanoparticles using a green synthesis method with an aqueous extract of date palm (Phoenix dactylifera) seeds as a natural reducing and stabilizing agent. The structural, morphological, magnetic, and biological properties of the synthesized particles were systematically analyzed. X-ray diffraction (XRD) confirmed the formation of a predominantly cubic spinel phase consistent with JCPDS card number 82-1049, with a characteristic peak at the (311) plane. Fourier transform infrared spectroscopy (FTIR) revealed vibrational bands for the Zn-O and Fe-O bonds at 563.71 and 438.97 cm^{-1}, respectively. The scanning electron microscopy (SEM) image showed irregularly shaped nanoparticles with an average diameter of 38.5 nm, as confirmed by size distribution analysis. Energy-dispersive X-ray spectroscopy (EDS) analysis revealed a Zn:Fe atomic ratio close to the expected stoichiometric value. Zeta potential measurements showed a value of (+11 mV), indicating limited colloidal stability with a moderately positive surface charge. A vibrating sample magnetometer (VSM) demonstrated superparamagnetic behavior with a saturation magnetization of 0.58 emu/g. Antibacterial activity assays using the agar diffusion method showed inhibition zones of 25 ± 0.6 mm against Staphylococcus aureus (ATCC 25923) and 19 ± 0.6 mm against Escherichia coli (ATCC 25922). Cell leakage assays confirmed that the primary mechanism of inhibition involves cell membrane disruption. Antioxidant activity showed an 82% inhibition at 0.6 µg/ml in the DPPH assay. These results indicate the promising potential of $ZnFe_2O_4$ nanoparticles derived from date seeds as a multifunctional nanomaterial for medical and environmental applications.

1 INTRODUCTION

Zinc ferrite ($ZnFe_2O_4$) is a magnetic nanomaterial belonging to the spinel group. It is characterized by a stable cubic crystal structure and advanced physical and chemical properties. This compound has garnered increasing attention in recent decades due to its numerous properties, such as catalytic activity, superior magnetic properties, and the ability to generate reactive oxygen species (ROS). These properties give it a prominent position among nanomaterials and open up avenues for its use in diverse applications, including medical, environmental, and industrial fields.

The need to develop effective nanomaterials has become urgent in light of contemporary health and environmental challenges, particularly with the widespread proliferation of bacteria resistant to traditional antibiotics. Nanomaterials, including $ZnFe_2O_4$, have demonstrated their ability to inhibit the growth of pathogenic bacteria such as Escherichia coli and Staphylococcus aureus through multiple mechanisms. These mechanisms include the generation of reactive oxygen species that damage bacterial proteins and DNA, the release of zinc and iron ions that interfere with bacterial biochemical processes, and direct interaction with the bacterial cell wall, leading to impaired membrane permeability and ionic imbalance. These combined mechanisms make $ZnFe_2O_4$ a promising material for medical applications as an antibacterial agent, for water treatment by inhibiting microbial growth, and for food preservation and shelf-life extension.

Conventional synthesis methods for zinc ferrite, including sol-gel, chemical precipitation, and spontaneous combustion, typically require high temperatures and toxic chemical solvents, raising environmental and health concerns and limiting their widespread application. This has led to the emergence of green synthesis as a safer and more sustainable alternative. Green synthesis utilizes plant extracts rich in phenolic compounds, flavonoids, and reducing sugars, which act as reducing agents and capping agents to form stable and environmentally friendly nanoparticles [1].

Among various natural resources, date seed extract represents a promising candidate for green synthesis due to its high antioxidant content, which facilitates the reduction of metal ions and stabilization of nanostructures [2], [3]. Furthermore, its abundant availability and low cost make it a sustainable resource that adds economic value to a previously neglected agricultural product [4], [5]. Utilizing date seeds in the preparation of $ZnFe_2O_4$ not only represents a step towards reducing environmental impact but also opens new avenues for investing local natural resources in the production of high-value-added nanomaterials. Despite the significant increase in research on the green synthesis of nanomaterials, the use of date seed extract for $ZnFe_2O_4$ synthesis has not been systematically investigated to our knowledge, and the relationship between structural composition and antibacterial properties remains insufficiently explored.

This study aims to synthesize $ZnFe_2O_4$ particles by green synthesis using date seed extract, to study their structural and morphological properties, and to evaluate their antibacterial efficacy against pathogenic strains, while presenting a sustainable strategy that combines high efficiency and an environmentally friendly approach for application in medical and environmental fields.

2 EXPERIMENTAL PART

2.1 Materials

All chemicals used in this study were of analytical grade and used without further purification. Sodium hydroxide (NaOH, micropearls) was obtained from RCI Labscan Limited. Zinc chloride ($ZnCl_2$, LR purity) and ferric chloride ($FeCl_3$, anhydrous) were purchased from Thomas Baker Chemicals Pvt. Ltd. Deionized water was used throughout the experiments. Date seeds were collected, cleaned, dried, and ground into fine powder for extract preparation.

2.2 Green Synthesis of $ZnFe_2O_4$ NPs

An aqueous extract of date seeds (1:10 w/v) was prepared by dispersing 10 g of dry date seed powder in 100 mL of distilled water. The mixture was then heated at 60-65 °C for 30 minutes with continuous stirring, followed by gradual cooling and filtration. The extract was then stored at 4 °C for later use. For nanoparticle synthesis, 0.02 mol of iron chloride ($FeCl_3$), equivalent to 3.244 g, and 0.01 mol of zinc chloride ($ZnCl_2$), equivalent to 1.363 g, were dissolved in 200 mL of deionized water at 60 °C with continuous stirring until a clear solution was obtained. Subsequently, 60 mL of the date seed extract was added dropwise under constant stirring at room temperature, resulting in the formation of a black precipitate. The pH of the mixture was gradually adjusted to 10 using dilute sodium hydroxide solution with continuous stirring, and then the mixture was stirred for an additional 30-60 min at room temperature. The resulting precipitate was separated by centrifugation at 4000 rpm and washed several times with deionized water, then dried at 70 °C for 3 hours. Finally, the dried powder was calcined in an oven at 400 °C for 4 hours and then allowed to cool gradually inside the oven to obtain $ZnFe_2O_4$ nanoparticles.

2.3 Characterization

The properties of zinc ferrite ($ZnFe_2O_4$) were investigated using a suite of advanced analytical instruments to ensure a comprehensive characterization of its structure, composition, and functional properties. X-ray diffraction (XRD, Rigaku Ultima IV) was used to determine the crystal structure and confirm phase purity. Infrared spectroscopy (FTIR, Thermo AVATAR) was performed to identify functional groups associated with the particle surface. For morphology and surface characterization, field-emission scanning electron microscopy (FESEM/EDX, TESCAN Mira3, Czech Republic) was used. Additionally, the zeta potential was measured using a Nanoparticle Analyzer (SZ-100V2, HORIBA, Japan) to determine the stability of the nanoparticles in an aqueous medium. Finally, the magnetic properties were evaluated using a vibratory sample magnetometer (VSM, Lake Shore Cryotronics 8600 Series, USA).

2.4 Antibacterial activity

2.4.1 Agar well Diffusion Assay

Bacterial culture procedures were performed according to previously published studies, with some minor modifications [6]. Bacterial strains from the American Strain Collection (ATCC) were used. Bacteria were cultured on nutrient agar (NA) and incubated at 37°C for 24 hours to obtain fresh and viable colonies. Subsequently, one colony was transferred to nutrient broth (NB) and incubated overnight at 37°C with agitation to achieve exponential growth. The optical density of the bacterial suspension was adjusted to match the McFarland standard of 0.5 (~1.5×10^8 CFU/mL).

Mueller-Hinton (MHA) agar plates were prepared and sterilized, and their surfaces were homogeneously inoculated using sterile swabs dipped in the bacterial suspensions. Wells (6 mm diameter) were created in the agar using a sterile cork drill. $ZnFe_2O_4$ nanoparticles were prepared in sterile distilled water at concentrations ranging from 75 to 100 µg/mL, and 100 mL of each concentration was added to the wells. Sterile distilled water was also used as a negative control. The plates were then incubated at 37 °C for 24 hours [7]-[9].

2.4.2 Release of Cellular Materials

Cellular release was assessed using sterile peptone water (0.75 g/mL), sterilized at 121 °C and 15 psi for 15 minutes. After incubating the bacterial strains for 24 hours, a 100 µg/mL solution of $ZnFe_2O_4$ nanoparticles was added to the tubes. Following treatment, the cells were centrifuged at 3500 rpm for specified time intervals (0, 30, 60, and 120 minutes). Spectral absorbance was measured at 260 nm, and the results are presented as the percentage change in absorbance compared to the initial values for each time interval [10].

2.4.3 Antioxidant Activity

The 2,2-diphenyl-1-picrylhydrazyl radical (DPPH) utilizes its antioxidant activity against $ZnFe_2O_4$ nanoparticles. When DPPH compounds react with antioxidant compounds, the ratios are reduced to the original value, noting that it has a characteristic absorption peak at 517nm.DPPH solutions were prepared by adding methanol (CH_3OH) at different concentrations. DPPH in methanol without the addition of an eye was used as the negative control, while ascorbic acid was used as the reference standard. The following selection ratio was calculated [11], [12]:

$$\text{Percent Inhibition} = \frac{A-B}{A} \times 100. \quad (1)$$

The empty solution (A) represents the absorbance of the DPPH solution in methanol without the composite nanocoating, while the sample solution (B) shows the absorbance of the DPPH solution with the composite nanofilm. The antioxidant activity was calculated by subtracting the value of B from the value of A.

3 RESULTS AND DISCUSSION

3.1 X-ray Diffraction Analysis

The X-ray diffraction (XRD) pattern of the sample showed distinct peaks at approximately 2θ = 28°, 32°, 47°, 56°, 63°, and 68°, corresponding to the (220), (311), (400), (511), (440), and (533) crystal planes, respectively (Fig. 1). These reflections are in good agreement with the standard data reported in JCPDS card No. 82-1049, confirming the formation of $ZnFe_2O_4$ with a cubic spinel structure [13]. Among the observed peaks, the (311) is the most intense and characteristic of this crystalline phase. The sharp and well-defined diffraction peaks suggest a high degree of crystallinity of the synthesized nanoparticles. Furthermore, the noticeable broadening of the diffraction peaks indicates the formation of particles on the nanometer scale. The analysis also showed that the average crystallite size was 21nm according to the Debye-Scherrer equation. These findings are consistent with previously reported studies on green-synthesized $ZnFe_2O_4$ nanoparticles and successful formation of crystalline spinel ferrite suitable for potential applications in antibacterial and catalytic systems [14], [15].

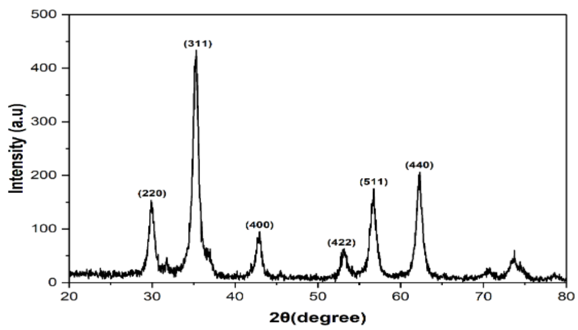

Figure 1: XRD of $ZnFe_2O_4$ NPs.

3.2 FTIR Analysis

The Fourier transform infrared (FTIR) spectra of $ZnFe_2O_4$ nanoparticles revealed distinct absorption bands, which were used to confirm their spinel ferrite structure, as shown in Figure 2 [16], [17]. A broad absorption band centered around 3284 cm^{-1} was attributed to the stretching vibrations of the O-H hydroxyl group adsorbed on the particle surface. The band at 1361 cm^{-1} was attributed to the bending vibrations of the O-H group, supporting the presence of adsorbed water on the particle surface. The peaks at 563 cm^{-1} and 438 cm^{-1} were attributed to the fundamental stretching vibrations of the Zn-O bonds at the tetrahedral and Fe-O bonds at the octahedral positions, respectively. These bands confirm the spinel structure of zinc ferrite $ZnFe_2O_4$. Furthermore, the presence of hydroxyl groups on the surface of nanoparticles is important in biological applications, as it can improve particle dispersion in aqueous environments and enhance their interaction with bacterial cell membranes. In addition to the intrinsic properties of $ZnFe_2O_4$ nanoparticles, such as the generation of reactive oxygen species (ROS) and the release of metal ions, surface hydroxyl groups may contribute to the observed antibacterial activity against S. aureus and E. coli [18], [19].

For comparison, the FTIR spectrum of the date seed extract Figure 2 shows a broad peak at ~3422 cm^{-1} corresponding to O-H stretching vibrations of phenolic compounds. The peaks at 2924 and 2855 cm^{-1} are attributed to C-H stretching vibrations, while the band at 1744 cm^{-1} corresponds to C=O stretching of carbonyl groups. Additional peaks at 1611, 1445, 1251, and 1052 cm^{-1} indicate the presence of aromatic rings, phenolic groups, and carbohydrates. These functional groups are known to play a crucial role in green synthesis, acting as reducing and stabilizing agents during nanoparticle formation. Their presence suggests that biomolecules from the date seed extract may have facilitated the formation and stabilization of $ZnFe_2O_4$ nanoparticles.

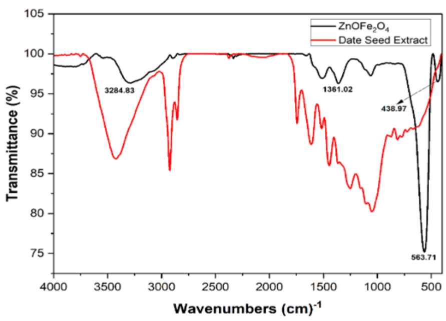

Figure 2: FTIR of $ZnFe_2O_4$ NPs.

3.3 SEM and EDS Analysis

Scanning electron microscopy (SEM) revealed that the synthesized $ZnFe_2O_4$ nanoparticles exhibit an irregular morphology with noticeable agglomeration, attributed to their nanoscale nature and high surface energy, which leads to adhesion during the preparation process. The observed morphology suggests that the green synthesis route influences particle growth and aggregation behavior, resulting in non-uniform nanoclusters. Structurally, the sample was analyzed using energy-dispersive X-ray spectroscopy (EDS) coupled with SEM, as shown in Figure 3. The results confirmed the presence of zinc (Zn), iron (Fe), and oxygen (O) as the primary constituents of the sample. No additional elements were detected within the sensitivity limits of the technique, suggesting the absence of significant impurities. Quantitative results also showed that the atomic ratio between Zn and Fe is close to 1:2, which is the ideal ratio for the chemical formula of $ZnFe_2O_4$, confirming the successful preparation and correct formation of the zinc ferrite, consistent with previous literature [20], [21].

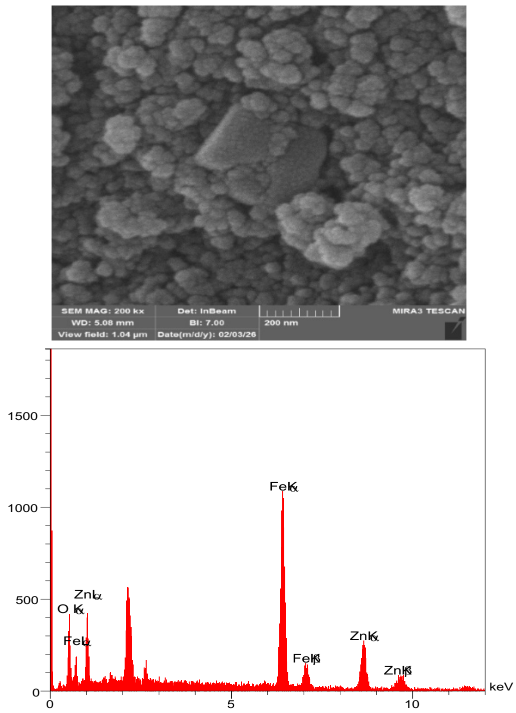

Figure 3: SEM image and EDS result of $ZnFe_2O_4$.

In addition to the morphological and structural analysis results, Figure 4 shows the histogram of the particle size distribution of the prepared $ZnFe_2O_4$. It reveals that most particles fall within a narrow nanoscale range, with an average diameter of approximately 38.5 nm, consistent with the SEM image observations that showed irregular nanoclusters. This distribution confirms that the green synthesis method contributed to the production of relatively homogeneous nanoparticles, further supporting the sample purity demonstrated by EDS analysis. The combination of the SEM/EDS results and the histogram demonstrate the successful preparation of a pure nanoscale morphology consistent with the ideal chemical structure of $ZnFe_2O_4$.

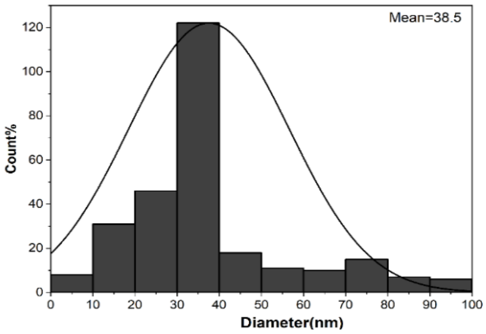

Figure 4: Size histogram of $ZnFe_2O_4$ NPs.

3.4 Zeta Potential Analysis

Zeta potential measurements of the $ZnFe_2O_4$ nanoparticles (Fig. 5) exhibited a relatively narrow distribution with an average value of approximately +11.0 mV, indicating that the particles possess a moderately positive surface charge. This value suggests limited electrostatic stabilization, as zeta potential values below ±30 mV is generally associated with reduced colloidal stability and a tendency toward particle aggregation. The relatively narrow distribution of zeta potential values reflects a degree of uniformity in surface charge among the nanoparticles; however, it does not necessarily imply monodispersity in particle size. The observed positive surface charge may be attributed to the adsorption of residual biomolecules from the date seed extract or surface hydroxyl groups formed during synthesis. This behavior is indicative of the particles' biocompatibility, as the positive charge facilitates their attraction to negatively charged bacterial membranes, promoting direct interaction and disrupting the cell membrane. This explains the observed antibacterial activity against both Staphylococcus aureus and Escherichia coli [22], [23].

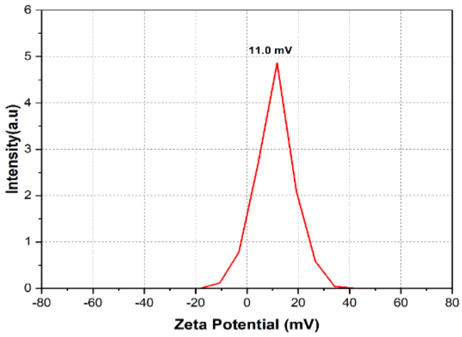

Figure 5: Zeta potential measurements of $ZnFe_2O_4$.

3.5 VSM Measurement

The magnetic properties of the synthesized $ZnFe_2O_4$ nanoparticles were investigated using a vibrational sample magnetometer (VSM) at room temperature in an applied field range of ±10,000 Oersted, as shown in Figure 6. The resulting M-H curve exhibited linear behavior passing through the origin without any obvious hysteresis loop, indicating the absence of residual magnetization ($Mr \approx 0$ emu/g) and coercivity ($Hc \approx 0$ Oe). These properties demonstrate superparamagnetic behavior, which is typical of nanoparticles below the critical size for single-domain size. The saturation magnetization (Ms) reached approximately 0.58 emu/g at an applied field of 10,000 Oersted. The low Ms value is attributed to the non-magnetic nature of the Zn^{2+} ions, which preferentially occupy the tetrahedral (A) sites in the spinel structure. This disrupts the super-exchange interactions between sites of tetrahedral (A) and octahedral (B) and reduces the overall magnetic moment. These results are consistent with previously reported values for green-synthesized $ZnFe_2O_4$ particles and confirm the potential of this material in biomedicine and related applications [24], [25].

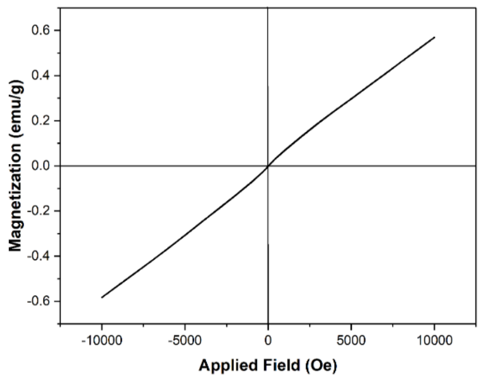

Figure 6: VSM of $ZnFe_2O_4$ NPs.

3.6 Antibacterial Properties of ZnFe2O4 NPs

The antibacterial activity of the synthesized $ZnFe_2O_4$ nanoparticles was evaluated against both Gram-negative (Escherichia coli) and Gram-positive (Staphylococcus aureus) bacteria using the agar well diffusion method. The data were interpreted by measuring the Zone of Inhibition (ZOI). Studies have shown that $ZnFe_2O_4$ nanoparticles inhibit the growth of several bacteria, including S. aureus and E. coli. As shown in Figure 7, the ZOIs reached 19 (±0.6) mm for E. coli and 25 (±0.6) mm for S. aureus, indicating higher activity against Gram-positive bacteria [26], [27]. The structural composition of $ZnFe_2O_4$ nanoparticles is the primary factor influencing their antibacterial activity. The antibacterial activity of $ZnFe_2O_4$ nanoparticles can be attributed to multiple mechanisms. One of the primary factors is the release of metal ions, such as Zn^{2+} and Fe^{3+}, which can interfere with essential cellular processes, including enzyme function and ion transport. Since antibacterial properties depend on stability and size, particle size significantly impacts antibacterial activity. Previous studies have shown that antibacterial activity increases with smaller particle size. Therefore, the $ZnFe_2O_4$ nanoparticles produced in the current study exhibit enhanced antibacterial activity. Their small size allows them to easily penetrate and destroy bacterial cells [28].

The electrostatic reactions caused by zinc ions released from $ZnFe_2O_4$ nanoparticles damage bacterial cell membranes. The antibacterial effect of these particles is due to their small size, which allows them to penetrate bacterial cells. The generation of reactive oxygen species (ROS) is a key antibacterial mechanism, including hydroxyl radicals (OH), superoxide anions (O_2^-), and hydrogen peroxide (H_2O_2) [29]. These reactive species can damage bacterial cell membranes, DNA, proteins, and other essential biomolecules, leading to cell death. Furthermore, $ZnFe_2O_4$ nanoparticles can directly interact with the lipid bilayer of bacterial cell membranes, leading to increased membrane permeability, leakage of cell contents, and disruption of ion exchange and homeostasis. Additionally, reactive oxygen species and metal ions can directly cause DNA cleavage, strand breaks, or oxidative modifications of its bases, inhibit bacterial replication and ultimately resulting in cell death [30], [31]. These results highlight that $ZnFe_2O_4$ nanoparticles not only exhibit antibacterial activity under laboratory conditions but also have promising potential for medical and environmental applications, particularly in combating antibiotic-resistant bacterial infections, making them a strategic option in developing more effective and safer future treatments.

3.7 Cellular Leakage Test

To confirm the antibacterial mechanism of $ZnFe_2O_4$ nanoparticles, a cellular leakage test was performed to assess the extent of cell membrane damage caused by these particles in S. aureus and E. coli bacteria. This test is based on the principle that damaged bacterial cell membranes lose their selective permeability, leading to leakage of the cell's internal contents, particularly nucleic acids and proteins, which can be measured spectroscopically at wavelengths of 260 nm [32]. As shown in Figures 8 and 9, the results demonstrated a progressive increase in absorbance at 260 nm in bacterial suspensions treated with $ZnFe_2O_4$ nanoparticles, depending on their concentration, indicating significant leakage of nucleic acids from both bacterial strains [33].

It is worth noting that $ZnFe_2O_4$ nanoparticles possess a unique magnetic property, belonging to the class of ferrite materials with a spinel structure that imparts significant magnetic properties. Furthermore, these particles may generate reactive oxygen species (ROS) that accelerate bacterial membrane degradation and exacerbate leakage of cellular contents [33], [34].

The degree of cellular leakage was significantly higher in S. aureus compared to E. coli, consistent with the antibacterial activity findings. This difference may be attributed to the structural variation between Gram-positive and Gram-negative bacteria. S. aureus bacteria, lacking an outer membrane, are more susceptible to nanoparticle penetration and damage to their cell membrane [35].

3.8 Antioxidant Activity of ZnFe2O4

The antioxidant activity of $ZnFe_2O_4$ nanoparticles was evaluated using the DPPH free radical scavenging assay, with vitamin C as a reference standard [36]. The assay was conducted within a concentration range of 0.1-0.6 µg/mL, and the results showed a gradual increase in inhibition percentages with increasing concentration [37]. At the lowest concentration (0.1 µg/mL), the inhibition percentage was low, reflecting limited initial activity. It then gradually increased at concentrations of 0.2 and 0.4 µg/mL, indicating a greater capacity to donate electrons or hydrogen atoms. At the highest concentration (0.6 µg/mL), the inhibition percentage reached 82%, confirming the potent free radical scavenging activity of these particles [38]. As illustrated in Figure 10, this upward trend highlights the dose-dependent behavior of $ZnFe_2O_4$ particles, reflecting their increasing ability to reduce DPPH molecules and change the solution's color from dark purple to yellow. This efficiency is attributed to the dual role of the bio-coating material on the particle surface, coupled with a stable spinel structure that imparts physicochemical properties conducive to redox reactions, making them promising candidates for biomedical applications such as anti-oxidative stress therapy, drug delivery, and bioimaging [39]-[41]. In addition to its high thermal and oxidative stability, it makes a promising candidate for biomedical applications such as oxidative stress therapy, drug delivery, bioimaging, and thermotherapy. Achieving an 82% inhibition rate at the highest concentration confirms its potential as a multifunctional nanomaterial with sustained activity and a low degradation rate within the biological environment [42]-[48].

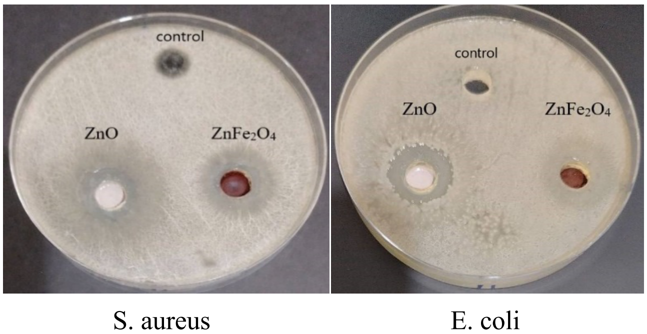

Figure 7: Antibacterial properties of ZnFe2O4 NPs against S. aureus and E. coli.

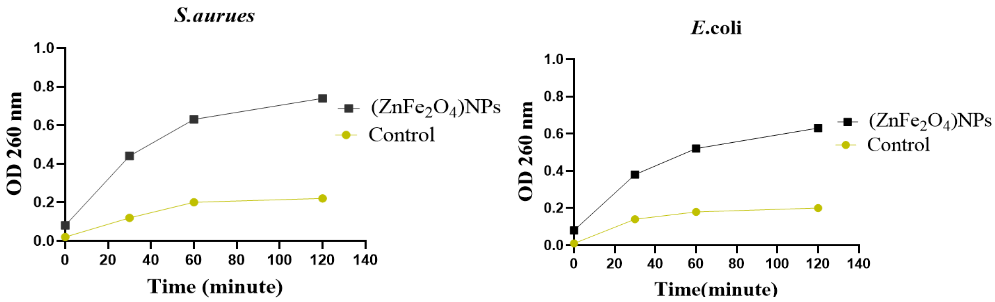

Figure 8: The effect of $ZnFe_2O_4$ nanoparticles on the release of cellular components of S.aureus and E. coli bacteria.

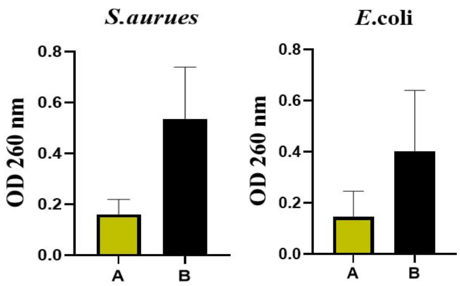

Figure 9: Effect of $ZnFe_2O_4$ nanoparticles, (A) control and (B) $ZnFe_2O_4$ NPs, on the release of cellular components of S. aureus and E. coli bacteria. Values are shown as mean ± standard error (SEM).

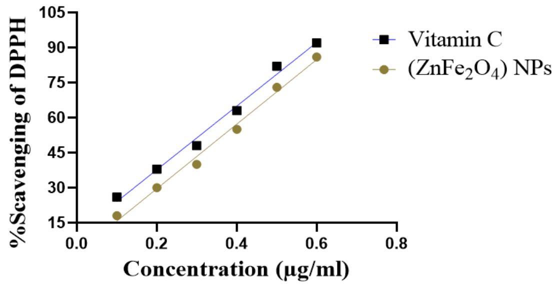

Figure 10: Antioxidant activity of $ZnFe_2O_4$ NPs.

4 CONCLUSIONS

This research presents the synthesis of $ZnFe_2O_4$ nanoparticles using a simple and efficient green synthesis method relying on date seed extract as a natural source of reduction and stabilization. Structural characterization revealed the formation of a crystalline spinel structure. X-ray diffraction (XRD) confirmed the single-phase structure, while Fourier transform infrared spectroscopy (FTIR) demonstrated the characteristic Zn-O and Fe-O bonds associated with the spinel lattice. Scanning electron microscopy (SEM) images showed irregular morphology with an average size of approximately 38.5 nm, and using energy-dispersive X-ray spectroscopy (EDS) confirmed a Zn:Fe ratio close to the expected stoichiometric composition. Zeta potential measurements also revealed a low positive surface charge (+11mV), suggesting limited colloidal stability but potential for interaction with negatively charged biological surfaces. VSM measurements revealed superparamagnetic behavior with a saturation magnetization of 0.58 emu/g, consistent with nanoscale ferrite materials [49]-[51].

Biological assessments demonstrated significant antibacterial activity against both Staphylococcus aureus and Escherichia coli, with inhibition zones of 25 ± 0.6 mm and 19 ± 0.6 mm, respectively, with greater efficacy against Gram-positive bacteria. Cell leakage assays confirmed that cell membrane disruption is a key inhibition mechanism, mediated by the generation of reactive oxygen species, the release of metal ions, and direct interaction between the nanoparticles and the membrane. Furthermore, the nanoparticles exhibited strong antioxidant activity, achieving an 82% dose-dependent inhibition rate in the DPPH assay at a concentration of 0.6 µg/mL. Overall, the results indicate that date seed extract is an efficient and sustainable source for the green synthesis of $ZnFe_2O_4$ nanoparticles with multifunctional properties. The combination of antibacterial activity, antioxidant activity, and superparamagnetic behavior makes these particles strong candidates for future medical applications, including antimicrobial therapy, targeted drug delivery, and bioimaging, thus supporting the development of sustainable nanotechnology.

REFERENCES

[1] R. Panja et al., "Antibacterial Potential of Nanocrystalline Zinc-Cobalt Ferrite," Nanomaterials, vol. 15, no. 17, p. 1318, Aug. 2025, doi: https://doi.org/10.3390/nano15171318.

[2] P. Dokania, S. Maity, P. B. Patil, and A. Sarkar, "Isothermal and Kinetics Modeling Approach for the Bioremediation of Potentially Toxic Trace Metal Ions Using a Novel Biosorbent Acalypha wilkesiana (Copperleaf) Leaves," Appl. Biochem. Biotechnol., vol. 196, no. 5, pp. 2487-2517, May 2024, doi: https://doi.org/10.1007/s12010-023-04678-5.

[3] E. Ahmad, R. Yousef, A. Alzoubi, and N. Saad Al-Din, "Structural, electrical and sensing properties of ZnFe2O4 nanoceramics synthesized by solid-state reaction method," Baghdad Science Journal, Feb. 2025, doi: https://doi.org/10.21123/bsj.2024.11346.

[4] S. Alfei, G. C. Schito, A. M. Schito, and G. Zuccari, "Reactive Oxygen Species (ROS)-Mediated Antibacterial Oxidative Therapies: Available Methods to Generate ROS and a Novel Option Proposal," Int. J. Mol. Sci., vol. 25, no. 13, p. 7182, Jun. 2024, doi: https://doi.org/10.3390/ijms25137182.

[5] W. K. Abdulkadhim, M. A. Mohammed, and A. Alasadi, "Superparamagnetic Fe3O4 nanoparticles capped with silver induce apoptosis of colon cancer cells via damaging DNA@increasing ROS," Nano-Structures & Nano-Objects, vol. 39, p. 101256, Sep. 2024, doi: https://doi.org/10.1016/j.nanoso.2024.101256.

[6] M. W. Alam, N. Dhanda, H. H. Almutairi, N. S. Al-Sowayan, S. Mushtaq, and S. A. Ansari, "Green Ferrites: Eco-Friendly Synthesis to Applications in Environmental Remediation, Antimicrobial Activity, and Catalysis-A Comprehensive Review," Appl. Organomet. Chem., vol. 39, no. 2, Feb. 2025, doi: https://doi.org/10.1002/aoc.7962.

[7] A. S. Abreu et al., "Evaluation of the Potential Carrier and Controlled Release of Antibiotics by Zinc, Nickel, and Cobalt Ferrite Nanoparticles Encapsulated with Silica and Functionalized with Moxifloxacin Hydrochloride," Particle & Particle Systems Characterization, Dec. 2025, doi: https://doi.org/10.1002/ppsc.202500167.

[8] R. Haghniaz et al., "Anti-bacterial and wound healing-promoting effects of zinc ferrite nanoparticles," J. Nanobiotechnology, vol. 19, no. 1, p. 38, Feb. 2021, doi: https://doi.org/10.1186/s12951-021-00776-w.

[9] D. Franco, G. Calabrese, S. P. P. Guglielmino, and S. Conoci, "Metal-Based Nanoparticles: Antibacterial Mechanisms and Biomedical Application," Microorganisms, vol. 10, no. 9, p. 1778, Sep. 2022,

doi: https://doi.org/10.3390/microorganisms10091778.

[10] N. T. T. Nguyen, T. T. T. Nguyen, D. T. C. Nguyen, and T. Van Tran, "Green synthesis of ZnFe2O4 nanoparticles using plant extracts and their applications: A review," Science of The Total Environment, vol. 872, p. 162212, May 2023, doi: https://doi.org/10.1016/j.scitotenv.2023.162212.

[11] J. Garg et al., "Emerging Trends in Zinc Ferrite Nanoparticles for Biomedical and Environmental Applications," Appl. Biochem. Biotechnol., vol. 196, no. 2, pp. 1008-1043, Feb. 2024, doi: https://doi.org/10.1007/s12010-023-04570-2.

[12] O. U. Modupe et al., "Green hydrothermal synthesis of nickel and zinc-doped nickel ferrite nanoparticles using Dalbergiella welwitschii extracts and their biological studies," Heliyon, vol. 11, no. 1, p. e40759, Jan. 2025, doi: https://doi.org/10.1016/j.heliyon.2024.e40759.

[13] M. S. Akhtar et al., "Green synthesis of magnetite iron oxide nanoparticles using Azadirachta indica leaf extract loaded on reduced graphene oxide and degradation of methylene blue," Sci. Rep., vol. 14, no. 1, p. 18172, Aug. 2024, doi: https://doi.org/10.1038/s41598-024-69184-y.

[14] M. El-Saadony et al., "Green Synthesis of Zinc Oxide Nanoparticles: Preparation, Characterization, and Biomedical Applications - A Review," Int. J. Nanomedicine, vol. 19, pp. 12889-12937, Dec. 2024, doi: https://doi.org/10.2147/IJN.S487188.

[15] S. Iravani, "Green synthesis of metal nanoparticles using plants," Green Chemistry, vol. 13, no. 10, p. 2638, 2011, doi: https://doi.org/10.1039/c1gc15386b.

[16] Himanshu, N. Kumar, I. Khangwal, and A. Upadhyay, "Assessment of nutritional composition, phytochemical screening, antioxidant, and antibacterial activities of date palm (Phoenix dactylifera) seeds," Discover Food, vol. 4, no. 1, p. 151, Nov. 2024, doi: https://doi.org/10.1007/s44187-024-00234-0.

[17] A. A. Halabi, B. H. Elwakil, M. Hagar, and Z. A. Olama, "Date Fruit (Phoenix dactylifera L.) Cultivar Extracts: Nanoparticle Synthesis, Antimicrobial and Antioxidant Activities," Molecules, vol. 27, no. 16, p. 5165, Aug. 2022, doi: https://doi.org/10.3390/molecules27165165.

[18] S. M. Ammar, "Date (Phoenix dactylifera L.) fruits and seeds nanotechnology: A mini review," Food systems, vol. 8, no. 2, pp. 231-234, Jul. 2025, doi: https://doi.org/10.21323/2618-9771-2025-8-2-231-234.

[19] M. E. Abdel-Alim, K. Samaan, D. Guillaume, and H. Amla, "Green Synthesis of Silver Nanoparticles using Egyptian Date Palm (Phoenix dactylifera L.) Seeds and Their Antibacterial Activity Assessment," Bioactivities, vol. 1, no. 1, pp. 1-8, Jun. 2023, doi: https://doi.org/10.47352/bioactivities.2963-654X.180.

[20] A. H. Phakatkar, P. Ghildiyal, Y. Wang, M. R. Zachariah, T. Shokuhfar, and R. Shahbazian-Yassar, "In-Situ TEM Studies on Nanoparticle Interactions with Bacterial Cells," Microscopy and Microanalysis, vol. 28, no. S1, pp. 1104-1106, Aug. 2022, doi: https://doi.org/10.1017/S1431927622004676.

[21] R. M. El-Masry et al., "Evaluation of the Antimicrobial Activity of ZnO Nanoparticles against Enterotoxigenic Staphylococcus aureus," ., vol. 12, no. 10, p. 1662, Oct. 2022, doi: https://doi.org/10.3390/life12101662.

[22] K. S. Khashan, B. A. Badr, G. M. Sulaiman, M. S. Jabir, and S. A. Hussain, "Antibacterial activity of Zinc Oxide nanostructured materials synthesis by laser ablation method," J. Phys. Conf. Ser., vol. 1795, no. 1, p. 012040, Mar. 2021, doi: https://doi.org/10.1088/1742-6596/1795/1/012040.

[23] M. A. Mohammed et al., "Magnetically enhanced ZnFe2O4 nanocomposite: a promising antibacterial, and antioxidant strategies," J. Solgel Sci. Technol., vol. 115, no. 3, pp. 1557-1566, Sep. 2025, doi: https://doi.org/10.1007/s10971-025-06870-x.

[24] N. Yang et al., "Magnesium implants with alternating magnetic field-enhanced hydrogen release and proton depletion for anti-infection treatment and tissue repair," Bioact. Mater., vol. 38, pp. 374-383, Aug. 2024, doi: https://doi.org/10.1016/j.bioactmat.2024.05.010.

[25] S. Venkataramaiah, M. M. Venkatappa, R. Rangappa, C. Udagani, and D. Sannaningaiah, "Green fabricated bimetallic zinc ferrite nanoparticles mitigate oxidative stress-induced pathogenesis," Anal. Biochem., vol. 700, p. 115767, May 2025, doi: https://doi.org/10.1016/j.ab.2025.115767.

[26] W. K. Abdulkadhim, A. B. Sahi, and M. A. Mohammed, "Gold-capped Fe3O4 nanoparticles with a magnetic field by damaging their DNA and generating more oxygen radicals, colon cancer cells can be made to die," Journal of Theoretical and Applied Physics, vol. 18, no. Special Issue, 2024, doi: https://doi.org/10.57647/j.jtap.2024.si-AICIS23.09.

[27] J. A. A. Abdullah et al., "Sustainable synthesis of ZnO and FexOy nanoparticles and their nanocomposite ZnFe2O4: Comprehensive characterization and applications in antioxidant activity and antibiotics degradation efficiency," Bioorg. Chem., vol. 153, p. 107828, Dec. 2024, doi: https://doi.org/10.1016/j.bioorg.2024.107828.

[28] A. A. Rasheed-Adeleke, O. C. Olatunde, N. H. Seheri, O. A. Oyewo, H. Ferjani, and D. C. Onwudiwe, "Synthesis and photocatalytic performance of ZnFe2O4 on the degradation of tetracycline in water," Applied Physics A, vol. 131, no. 8, p. 625, Aug. 2025, doi: https://doi.org/10.1007/s00339-025-08753-y.

[29] M. M. El-Masry and M. M. Arman, "Cobalt, nickel and zinc spinel ferrites with high transmittance and UV-blocking for advanced optical applications.," Sci. Rep., vol. 15, no. 1, p. 16636, May 2025, doi: https://doi.org/10.1038/s41598-025-99604-6.

[30] A. C. Murrieta, D. Cavazos-Cavazos, C. Flores-Jauregui, P. Sepúlveda, M. Hesiquio-Garduño, and F. F. Contreras-Torres, "Characterization of hydrothermally synthesized ZnFe2O4 spinel ferrite: Insights into microstructure, inversion degree, and crystal evolution," Journal of Physics and Chemistry of Solids, vol. 183, p. 111659, Dec. 2023, doi: https://doi.org/10.1016/j.jpcs.2023.111659.

[31] T. Sarkar, S. Kundu, G. Ghorai, P. K. Sahoo, V. R. Reddy, and A. Bhattacharjee, "Synthesis and characterization of zinc ferrite nanomaterials vis-à-vis studies on their photocatalytic application in visible light dye degradation," Applied Physics A, vol. 131, no. 4, p. 266, Apr. 2025, doi: https://doi.org/10.1007/s00339-025-08370-9.

[32] P. S. Patil, M. V. Khedkar, Y. P. Ubale, S. S. Gawali, and K. M. Jadhav, "Visible-light-responsive ZnFe2O4 nanocatalysts for enhanced hydrogen production via. photocatalytic water splitting," Journal of Materials Science: Materials in Electronics, vol. 36, no. 17, p. 1014, Jun. 2025, doi: https://doi.org/10.1007/s10854-025-15005-5.

[33] O. Bakina et al., "New PMMA-Based Hydroxyapatite/ZnFe2O4/ZnO Composite with Antibacterial Performance and Low Toxicity," Biomimetics, vol. 8, no. 6, p. 488, Oct. 2023, doi: https://doi.org/10.3390/biomimetics8060488.

[34] Z. Guo et al., "Study of antibacterial activity of copper zinc nanocomposites and disruption of bacterial cytoplasmic membrane," Sci. Rep., vol. 15, no. 1, p. 26780, Jul. 2025, doi: https://doi.org/10.1038/s41598-025-93691-1.

[35] D. Thakur, M. Latwal, J. P. Singh, L. K. Gupta, and R. C. Srivastava, "Zinc ferrite nanoparticles and their biomedical applications," in Oxides for Medical Applications, Elsevier, 2023, pp. 233-255, doi: https://doi.org/10.1016/B978-0-323-90538-1.00014-5.

[36] S. C. Chabattula et al., "Anti-cancer Application of Nat-ZnFe2O4 Nanoparticles on 2D Tumor Models," Appl. Biochem. Biotechnol., vol. 196, no. 2, pp. 1058-1078, Feb. 2024, doi: https://doi.org/10.1007/s12010-023-04582-y.

[37] S. H. Abed, R. A. Madhi, K. Heydaryan, and A. F. Shamkhi, "Green synthesis of gold-doped ZnFe2O4 nanoparticles using Crataegus monogyna leaf extract: characterization, antibacterial, and efficient degradation of methylene blue and eriochrome black T pollutants," Biomass Convers. Biorefin., vol. 15, no. 4, pp. 5631-5641, Feb. 2025, doi: https://doi.org/10.1007/s13399-024-05337-3.

[38] A. M. El-Khawaga, K. Elmaghraby, and M. Orlandini, "Amoxicillin conjugated functionalized zinc ferrite nanoparticles for enhanced antibacterial, antibiofilm, and antioxidant activities," Sci. Rep., vol. 15, no. 1, p. 24951, Jul. 2025, doi: https://doi.org/10.1038/s41598-025-08782-w.

[39] X. Zhou et al., "Synthesis and antibacterial properties of core-shell nano-ZnFe2O4@ZnS/Cu2S composites.," Journal of Environmental And Sciences, vol. 6, no. 1, pp. 1-17, Jan. 2019, doi: https://doi.org/10.52338/joes.2024.4052.

[40] S. Jiang, K. Lin, and M. Cai, "ZnO Nanomaterials: Current Advancements in Antibacterial Mechanisms and Applications," Front. Chem., vol. 8, Jul. 2020, doi: https://doi.org/10.3389/fchem.2020.00580.

[41] R. Singh, S. Cheng, and S. Singh, "Oxidative stress-mediated genotoxic effect of zinc oxide nanoparticles on Deinococcus radiodurans," 3 Biotech, vol. 10, no. 2, p. 66, Feb. 2020, doi: https://doi.org/10.1007/s13205-020-2054-4.

[42] P. Sahoo, P. Choudhary, S. S. Laha, A. Dixit, and O. T. Mefford, "Recent advances in zinc ferrite (ZnFe 2 O 4) based nanostructures for magnetic hyperthermia applications," Chemical Communications, vol. 59, no. 81, pp. 12065-12090, 2023, doi: https://doi.org/10.1039/D3CC01637D.

[43] R. P. Sharma, S. D. Raut, V. V. Jadhav, R. M. Mulani, A. S. Kadam, and R. S. Mane, "Assessment of antibacterial and anti-biofilm effects of zinc ferrite nanoparticles against Klebsiella pneumoniae," Folia Microbiol. (Praha)., vol. 67, no. 5, pp. 747-755, Oct. 2022, doi: https://doi.org/10.1007/s12223-022-00969-2.

[44] S. M. Sachin, G. Govindasamy, S. J. Sundaram, J. P. R. Fathima, and M. S. Nivetha, "Facile synthesis of zinc ferrite magnetic nanoparticles for antibacterial application," Nanotechnology for Environmental Engineering, vol. 10, no. 2, p. 34, Jun. 2025, doi: https://doi.org/10.1007/s41204-025-00430-y.

[45] A. M. El-Khawaga, M. Ayman, O. Hafez, and R. E. Shalaby, "Photocatalytic, antimicrobial and antibiofilm activities of MgFe2O4 magnetic nanoparticles," Sci. Rep., vol. 14, no. 1, p. 12877, Jun. 2024, doi: https://doi.org/10.1038/s41598-024-62868-5.

[46] Chaturvedi and R. Ranjan, "Antimicrobial nanoparticles: a new horizon to combat multidrug-resistant bacteria," Frontiers in Nanotechnology, vol. 7, Nov. 2025, doi: https://doi.org/10.3389/fnano.2025.1611126.

[47] İ. Gulcin and S. H. Alwasel, "DPPH Radical Scavenging Assay," Processes, vol. 11, no. 8, p. 2248, Jul. 2023, doi: https://doi.org/10.3390/pr11082248.

[48] S. Venkataramaiah, M. M. Venkatappa, R. Rangappa, C. Udagani, and D. Sannaningaiah, "Green fabricated bimetallic zinc ferrite nanoparticles mitigate oxidative stress-induced pathogenesis," Anal. Biochem., vol. 700, p. 115767, May 2025, doi: https://doi.org/10.1016/j.ab.2025.115767.

[49] M. Ye, Y. Zhou, H. Zhao, and X. Wang, "Magnetic Microrobots with Folate Targeting for Drug Delivery," Cyborg and Bionic Systems, vol. 4, Jan. 2023, doi: https://doi.org/10.34133/cbsystems.0019.

[50] J. Garg et al., "Emerging Trends in Zinc Ferrite Nanoparticles for Biomedical and Environmental Applications," Appl. Biochem. Biotechnol., vol. 196, no. 2, pp. 1008-1043, Feb. 2024, doi: https://doi.org/10.1007/s12010-023-04570-2.

[51] A. Rajan, S. S. Laha, N. K. Sahu, N. D. Thorat, and B. Shankar, "Recent advancements and clinical aspects of engineered iron oxide nanoplatforms for magnetic hyperthermia-induced cancer therapy," Mater. Today Bio, vol. 29, p. 101348, Dec. 2024, doi: https://doi.org/10.1016/j.mtbio.2024.101348.